Cracks in reinforced FRC beams subject to bending and axial load

J.F.Olesen
Department of Civil Engineering, Technical University of Denmark, Denmark

ABSTRACT: The development of bending cracks in fibre reinforced concrete (FRC) beams with main reinforcement bars is modelled applying the fictitious crack model. A beam subject to bending moment and normal force is modelled. Closed form solutions are given for the bending moment and crack opening, spacing and length; all functions of the cross-sectional rotation and the normal force. The model may be conceived as an adaptive hinge element, only considering the part of the beam, which is affected by the developing crack; this part defined by the length of reinforcement de-bonding. Constant friction is assumed between the de-bonded bar and the FRC. The stress-crack opening relationship, modelling the tensile behaviour of the FRC, is taken as a constant level instantly dropping from the uni-axial tensile strength, and the effect of fibres is studied by varying this post-peak stress level. Finally, the model is applied for the determination of beam deflections.

1 INTRODUCTION

Although the addition of fibres to concrete is known to enhance the performance of the resulting material, especially with respect to tensional behaviour, fibre reinforced concrete (FRC) is hardly ever used for structural elements. The reason for this is believed to be the lack of test methods and rigorous design methods based on consistent theoretical modelling and experimental verification. Test methods for the characterisation of FRC materials in tension, however, are not a subject of the present paper. Rather, the aim is to provide a consistent theoretical model for the development of bending cracks in structural FRC beams, i.e. conventionally reinforced beams cast with FRC.

Fibres in concrete add to the fracture energy of the FRC compound, and they are responsible for the substantial residual load carrying capacity in tension observed at fairly large crack opening values. Of course the performance very much depends on the type and amount of fibres added. The fibres counteract the opening of cracks, enabling the control of crack growth, and resulting in reduced crack widths as compared to similar cracks in conventional concrete structures.

The design of conventionally reinforced flexural concrete members is often governed by maximum crack width requirements in the serviceability limit state. The application of FRC could be an attractive alternative to conventional measures of fulfilling these requirements. Addition of fibres instead of in-creasing the amount of main reinforcement or beam depth could lead to more optimal designs in terms of beam dimensions and economy.

The approach taken here is based on non-linear fracture mechanics utilising a very simple post-peak model for the tensile softening behaviour of FRC: the post-peak stress is assumed to be at a constant level, defining the so-called toughness class of the FRC. Furthermore, the interaction between the main reinforcement bars and the surrounding FRC material is taken to be a constant interfacial shear stress. These simplifying assumptions allow for the development of closed form solutions for the description of the growth of bending cracks in main reinforced FRC beams with a rectangular cross-section.

From the analysis of the mean cross-sectional rotation as a function of the bending moment, given by the closed form solutions, it is demonstrated that the moment-rotation relationship essentially is bi-linear. Thus, it is shown that the behaviour in the post-crack regime is well described by the asymptotic linear solution valid for infinitely large rotations. This finding allows for the simple calculation of the beam deflection as a function of the moment distribution.

2 MATERIAL MODELS

The uni-axial tensile behaviour of concrete and fibre reinforced concrete is modelled within the concepts of the fictitious crack model, originally suggested by Hillerborg et al. (1976) for modelling concrete, and

later by Hillerborg (1980) for the description of crack formation in FRC. In this model the response of the material is assumed to be essentially linear until peak load at which point a discrete crack is assumed to initiate. The fundamental idea of the fictitious crack model is the assumption that the crack faces are not traction free, and that aggregates and fibres may transfer stresses across the crack opening. The magnitude of the transferred stress is modelled as a function of the crack opening, which is denoted by w. This function is known as *the stress-crack opening relationship*: $\sigma_w(w)$. Furthermore, the model assumes that the stress concentration at the crack tip is eliminated by the stresses on the crack faces such that the propagation of the crack is governed by the tensile strength f_t.

The stress-crack opening relationship may be determined in a direct uni-axial tension test, and it has been found that it is reasonably well described by a bi-linear curve (Stang & Olesen 1998). The first part of this curve describes the cracking of the concrete matrix whereas the second part relates to the de-bonding and pullout of fibres, see Figure 1.

Although the bi-linear stress-crack opening relationship is simple, it is not considered operational in a design situation. Therefore, a further simplification has been suggested by Stang & Olesen (2000). They simply assume that the stress transferred across the crack σ_w remains constant during crack opening. The magnitude of the transferred constant stress level is given as a fraction of the tensile strength according to

$$\sigma_w(w) = \gamma f_t \quad \text{for} \quad 0 < w < w^* \tag{1}$$

The fraction γ is called the toughness class and it is associated with a maximum crack opening w^*. The magnitude of γ reflects the effect of fibres, the more
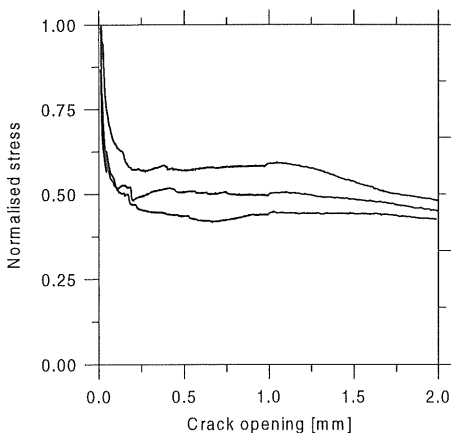

Figure 1. Stress-crack opening relationship normalised with respect to uniaxial tensile strength. Normal strength concrete with 1% by volume of steel fibres. Results of three tests.
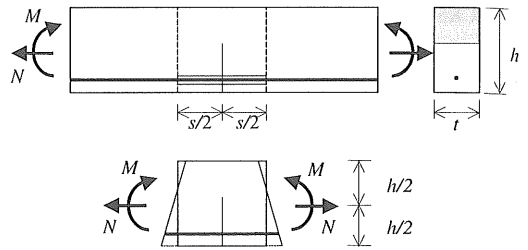

Figure 2. Beam model defining the geometry of the adaptive hinge element, the moment and axial loading and the overall hinge deformation.

fibres the larger the value of γ. The determination of γ may be based on the results of a simple bending test (Stang & Olesen 2000).

The behaviour of FRC in compression is mainly affected in the post-peak regime by the presence of fibres. Here, however, it is assumed that compressive stresses are well below the compressive strength, and that the behaviour in compression may be assumed to be linear elastic. Furthermore, the elastic modulus in tension is taken to be the same as in compression: E_c.

The reinforcement bars are assumed to behave linear elastic with an elastic modulus denoted by E_s. The interaction between a reinforcement bar and surrounding FRC is characterised either by a perfect bond or by interfacial friction with a constant shear stress τ. The de-bonding process is not considered, and thus, the de-bonding energy is disregarded.

3 ADAPTIVE HINGE ELEMENT

The basic ideas of the model to be presented here have previously been described for the case of pure bending (Olesen 2000). However, the present model has been extended to allow for a non-zero axial load to act simultaneously with the bending moment. This extension permits the application of the model to structures like beam-columns or post-tensioned beams.

Consider a prismatic FRC beam with a rectangular cross-section and reinforced with a main reinforcement bar placed in the mid-plane of the beam as shown in Figure 2. The beam is subject to a constant bending moment M around an axis perpendicular to the beam mid-plane and a constant axial load N acting in the mid-plane in the direction of the beam axis. Positive directions of the loads are defined in the figure. The beam may have a number of main bars, however, the model has only one reinforcing bar. More bars at the same depth may be considered just by adjusting the width of the model beam according to the number of bars, i.e. for a beam with two bars at the same level, the width of the model beam is set to half the width of the real

beam, and only one bar is taken into account. The dimensions of the beam cross-section are h and t denoting depth and width, respectively.

When the load on the beam is sufficiently small it responds in a linear elastic manner. At some load, however, the stress at the bottom face of the beam reaches the tensile strength, and a crack is initiated. This bending crack is assumed to penetrate upwards all across the cross-section, confined to the cross-sectional plane. When it reaches the main bar, the bar is assumed to de-bond from the FRC matrix allowing the bending crack to open and penetrate further upwards. The de-bonding length is determined by the shear stress acting on the de-bonded interfaces and by the length and width of the bending crack. However, at this point it is assumed that the total de-bonding length s is known.

The adaptive hinge element is defined as the part of the beam affected by the penetrating bending crack. The length of de-bonding gives this part of the beam, i.e. the hinge element extends $s/2$ to either side of the bending crack (Fig. 1). Since the de-bonding length is not a constant but a function of the load, the beam element must adapt itself accordingly. The vertical boundary lines of the element are assumed to remain straight during deformation. Moreover, the bar is assumed to have de-bonded throughout the length of the element while there is perfect bond at the element boundaries. Thus, the bar may be seen as attached to the vertical boundary lines and following these during deformation.

In Figure 3 the left half of the adaptive element is shown together with the stress distribution in the cracked mid-section of the element. Furthermore, the angle of rotation of the boundary line with respect to the mid-section line is introduced as φ; the depth of the neutral axis is introduced as y_0 and the depth of the bar as d_s. The crack length is denoted by c. In the cracked part of the mid-section the stress distribution is constant and given by Equation (1) according to the simple description of the tension softening behaviour of FRC. In the remaining part the stress varies linearly, and attains the tensile strength, f_t, at the crack tip.

We recall the assumption of a constant shear stress, τ, acting on the de-bonded surfaces. Thus, the interfacial shear stress per unit length T acting on the FRC and the reinforcement bar is given by $T = \pi D \tau$, where D is the diameter of the reinforcement bar. The static equivalent forces F_c account for the action of these shear stresses on the FRC, one force acting at the left boundary, and the other acting at the mid-section. This equivalent force is given by $F_c = Ts/4$ as shown in Figure 4.

The normal force in the reinforcement bar varies linearly due to the action of the interfacial shear; it increases linearly from the boundary towards the mid-section. At the left boundary it attains the value
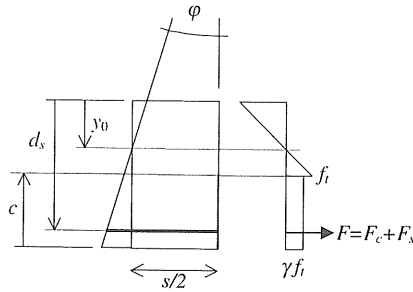

Figure 3. Left half of adaptive hinge element showing the normal stress distribution in the cracked mid-section in the FRC material. The normal force in the main reinforcement bar, F_s, is shown together with the concentrated force, F_c, accounting for the shear stress acting on the FRC material around the bar.
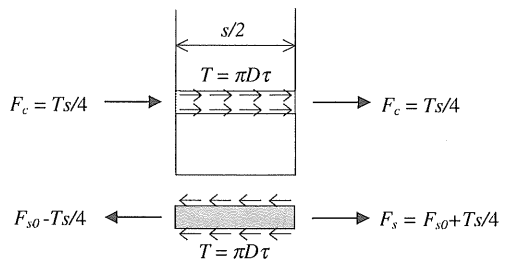

Figure 4. Left half of adaptive hinge element showing the interfacial shear (FRC and reinforcement bar drawn separately). F_c is the equivalent action of the shear stresses on the FRC material. F_s incorporates the action of the shear stresses into the normal force in the reinforcement bar at the cracked mid-section.

$F_{s0} - Ts/4$ and at the mid-section: $F_s = F_{s0} + Ts/4$, where F_{s0} is the mean normal force in the bar due to the deformation of the hinge element and given by

$$F_{s0} = \frac{2(d_s - y_0)\varphi}{s} E_s A_s \qquad (2)$$

where A_s denotes the cross-sectional area of the reinforcement bar.

At this point we may express the resulting normal force at the mid-section in terms of the depth of the neutral axis y_0 the hinge width s and the rotation angle φ. Thus, from the condition that the resulting normal force must equal the axial load N we may derive an expression for y_0 in terms of φ. Here it has been utilised that y_0, c and φ are related through:

$$c = h - y_0 - \frac{f_t s}{2E_c \varphi} \qquad (3)$$

The moment M of the sectional normal stresses and forces may now be calculated and expressed in terms of c and φ. It should be emphasised that the width of the hinge element, s, has only been as-

sumed to be known at this point. The following results for the crack length and the bending moment are expressed in normalised terms according to the following normalisations

$$\theta = \frac{hE_c}{sf_t}\varphi, \quad \alpha = \frac{c}{h}, \quad \mu = \frac{6M}{f_t h^2 t}, \quad \rho = \frac{N}{f_t ht} \quad (4)$$

where θ, α, μ and ρ are the normalised rotation, crack length, bending moment and axial force, respectively.

The result for the normalised crack length α is given by

$$\alpha(\theta,\rho) = 1 - \frac{1-\gamma}{2\theta} + \Phi$$
$$- \sqrt{\Phi\left(\Phi + 2\delta + \frac{\gamma}{\theta}\right) + \left(\frac{1-\gamma}{2\theta}\right)^2 + \frac{\gamma+\psi-\rho}{\theta}} \quad (5)$$

and the result for the normalised moment μ is given by

$$\mu(\alpha,\theta,\rho) =$$
$$4\Big[1 + 3\Phi(1-\delta)^2 - 3(1+2\Phi(1-\delta))\alpha$$
$$+ 3(1+\Phi)\alpha^2 - \alpha^3\Big]\theta + 6(\Phi+\psi+1-\rho)\alpha \quad (6)$$
$$- 3(1-\rho) + 3(\gamma-1)\alpha^2 - 6(\Phi+\psi)(1-\delta)$$

where the following symbols have been introduced

$$\Phi = \frac{E_s A_s}{E_c ht}, \quad \delta = \frac{d_s}{h}, \quad \psi = \frac{Ts}{2f_t ht} \quad (7)$$

to denote the mechanical reinforcement ratio, the relative depth of the reinforcement and the normalised interfacial shear force, respectively. Note that expressions given in (5) and (6) implicitly depend on the hinge width s.

The hinge element behaves linear elastic at small deformations. The elastic limit, θ_0, may be found by solving Equation (5) with respect to θ, demanding that $\alpha = 0$ and $\psi = 0$:

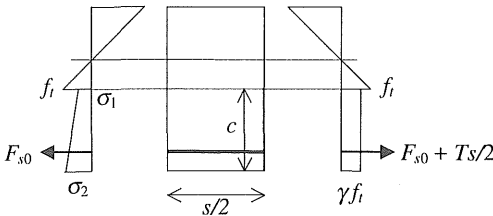$$\theta_0 = \frac{1+\Phi-\rho}{1+2(1-\delta)\Phi} \quad (8)$$

Figure 5. Left half of adaptive hinge element showing the assumed stress distribution at the left boundary line together with the stress distribution at the mid-section.

The normalised moment μ_0 corresponding to this elastic limit is given by

$$\mu_0 = \frac{(1-\rho) + \left[4 - (12\delta(1-\rho) + 6\rho)(1-\delta)\right]\Phi}{1+2(1-\delta)\Phi} \quad (9)$$

4 DE-BONDING LENGTH

The de-bonding length determines the size, s, of the adaptive hinge element. It enters into the expressions (5) and (6) through the parameter ψ given in (7), and at this point s has been assumed a known quantity. To determine the de-bonding length we look at the stress distribution in the adaptive hinge element. The shear interaction between the reinforcement bar and the FRC shifts load from the bar to the FRC as we move away from the crack face. The further away we move, the larger the stresses in the FRC. At some point away from the crack the stress at the bottom face reaches the value of the tensile strength, which cannot be exceeded. Since at this point a new crack may be initiated, the distance between this point and the cracked section determines the de-bonding length $s/2$.

Consider the left half of the hinge element and assume a stress distribution at the vertical element boundary line as shown in Figure 5. This stress distribution must be static equivalent with the stress distribution in the cracked mid-section, and expressions for σ_1 and σ_2 defining the lower linear part of the stress distribution, are readily obtained.

The condition which yields the de-bonding length, and thus the size of the hinge element, is that $\sigma_2 = f_t$, since σ_2 cannot exceed the tensile strength. From this condition the following expression is derived:

$$\psi = (1-\gamma)\frac{\alpha}{4}\frac{2\alpha}{2\alpha - 3(1-\delta)} \quad (10)$$

Since α is a function of ψ this equation implicitly establishes ψ and the total de-bonding length, s. However, a closed form solution is not obtainable. To overcome this problem we must accept the approximation $1-\delta \approx 0$, which is introduced into Equation (10) yielding

$$\psi = (1-\gamma)\frac{\alpha}{4} \quad (11)$$

Introducing (5) into (11) and solving with respect to ψ we get:

$$\psi = \frac{1-\gamma}{32\theta}\Big[8\theta(1+\Phi) - 3(1-\gamma) - \sqrt{K}\Big] \quad (12)$$

where K is given by

$$K = 64\Phi(\Phi+2\delta)\theta^2 + 16(1+3\gamma)(1+\Phi)\theta$$
$$+ 9(1-\gamma)^2 \quad (13)$$

The hinge solution is now fully established as a function of the independent variable θ, the normalised deformation and the normalised axial load ρ. For varying values of θ, first establish ψ from (12) and (13), then establish the normalised crack length α from (5), and finally, establish the normalised moment μ from (6).

5 CRACK OPENING

The crack opening at the bottom face of the beam, often called the crack mouth opening displacement $CMOD$, is determined as the difference between the geometrical elongation of the bottom face and the elastic extension. The geometrical elongation u_g is given by

$$u_g = 2\varphi(h - y_0) = (2\alpha\theta + 1)\frac{sf_t}{E_c} \tag{14}$$

The elastic extension u_e of the bottom face of the hinge element is determined by assuming a linear declination of stresses from f_t at the boundary to γf_t at the crack:

$$u_e = (1+\gamma)\frac{sf_t}{2E_c} \tag{15}$$

Thus,

$$CMOD = u_g - u_e = (2\alpha\theta + \frac{1-\gamma}{2})\frac{sf_t}{E_c} \tag{16}$$

6 BEAM DEFLECTION

The mean curvature κ of the hinge and thus of the beam is given by

$$\kappa = 2\frac{\varphi}{s} = \frac{2f_t}{hE_c}\theta \tag{17}$$

Now, if θ may be expressed in term of the normalised moment μ the deflection of the beam may be determined by integration of κ. In the elastic range, i.e. when $0 \le \theta \le \theta_0$, θ is given by

$$\theta = \theta_0 \frac{\mu}{\mu_0} \tag{18}$$

where θ_0 and μ_0 are given by (8) and (9), respectively. In the cracked non-linear range, i.e. when $\theta_0 < \theta$, it is not possible to isolate θ as a function of μ. However, an asymptotic expression may be derived, which is correct in the limiting case of θ approaching infinity. Although this expression is only correct in an asymptotic sense, the error made by applying it as an approximation to the relationship between μ and θ, is small even at small values of θ. Taking the

expression for ψ given in (12) and (13) to the limit $\theta \to \infty$ we find that

$$\psi \to \psi_\infty = \frac{1-\gamma}{4}\alpha_\infty \tag{19}$$

where α_∞ is the limit value of α found from taking (5) to the limit $\theta \to \infty$:

$$\alpha \to \alpha_\infty = 1 + \Phi - \sqrt{\Phi(\Phi + 2\delta)} \tag{20}$$

The limit expression for μ as $\theta \to \infty$ is found form expression (6), and we obtain the following linear relationship

$$\mu \to \mu_\infty = \mu_1\theta + \mu_2 \tag{21}$$

where

$$\mu_1 = 4\Phi\{3\delta(2\Phi + \delta) + 2\Phi^2 \\ - 2(\Phi + 2\delta)\sqrt{\Phi(\Phi + 2\delta)}\}$$

$$\mu_2 = \frac{3}{2}\{(3 + 4(\Phi - \rho) + \gamma + \delta - \gamma\delta)\alpha_\infty \\ - (1-\gamma)\alpha_\infty^2 - 4\Phi(1-\delta) - 2(1-\rho)\} \tag{22}$$

From the expression in (21) the following linear relation between θ and μ is readily obtained:

$$\theta = \frac{\mu - \mu_2}{\mu_1} \tag{23}$$

The elastic solution (18) is now extended until intersection with the asymptotic solution (23), and the point of intersection is given by $\mu = \mu^*$, where

$$\mu^* = \frac{\mu_0\mu_2}{\mu_0 - \theta_0\mu_1} \tag{24}$$

Thus, for $\mu \le \mu^*$ (18) applies, whereas for $\mu > \mu^*$ (23) applies. Now, if the distribution of the bending moment is known in every point of the beam, the curvature distribution may be found from (17), (18) and (23), and the overall deflection of the beam may be established.

7 SAMPLE BEAM

We consider a beam 200 mm wide and 350 mm deep, reinforced with two bars Ø20 mm placed 305 mm from the top, and loaded symmetrically in four point bending, i.e. $\rho = 0$. Only the middle part of the beam where the bending moment is constant is considered. The beam is cast with FRC characterised through the magnitude of the post crack stress level γ. The tensile strength of the FRC is assumed to equal 3 MPa and the elastic modulus 30 GPa. Finally, the elastic modulus of the bars is assumed to
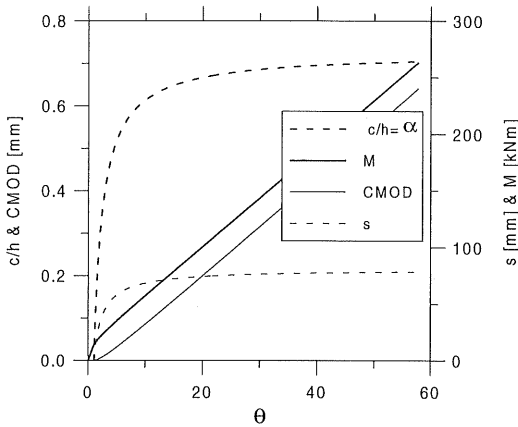
Figure 6. Results for the sample FRC beam ($\rho = 0$) with the toughness class $\gamma = 0.6$ as functions of the normalised hinge deformation, θ.

be 210 GPa and the interfacial shear stress is set to 3 MPa.

In Figure 6 the results for this sample beam with $\gamma = 0.6$ are presented. The calculations are straightforward, first s is calculated as a function of θ, then α and μ, and finally M and $CMOD$ are calculated. Note that the behaviour of M is almost bi-linear, indicating the suitability of the asymptotic approximation made in the previous section. This is remarkable considering the non-linearity of α and s. Also $CMOD$ is nearly linear, resulting in an almost linear relationship between moment and crack opening. This is illustrated in Figure 7 for different values of the toughness class γ. Increasing the amount of fibres in a FRC corresponds to increasing the toughness class. If there are no fibres at all, γ almost vanishes, whereas, a typical value of γ for a FRC with

1% by volume of commercial steel fibres in a normal strength concrete is 0.6-0.7. Thus, Figure 7 suggests that the crack opening in a FRC beam with 1% of fibres would be less than one third of the crack opening in a concrete beam without fibres, at the same load level.

Results from tests on beams similar to the above sample beam have recently been reported by Vandewalle (2000). However, a direct comparison with the model results is not feasible due to lack of information on fracture mechanics parameters. Nevertheless, a qualitative comparison of results is in support of the adaptive hinge model.

8 CONCLUSION

In order to describe the crack formation in a reinforced FRC beam, a so-called adaptive hinge model has been derived based on a non-linear fracture mechanics approach applying a very simple stress-crack opening relationship. From this model a bi-linear relationship is extracted which describes the flexibility of the beam enabling the determination of the beam deflection as a function of the moment distribution. The model incorporates the effects of a possible axial load. The validity of the adaptive hinge model has not yet been assessed through dedicated experiments; however, results for beams in pure bending published recently do not contradict the feasibility of the model, although the documentation is not sufficiently detailed to perform comparable model studies.
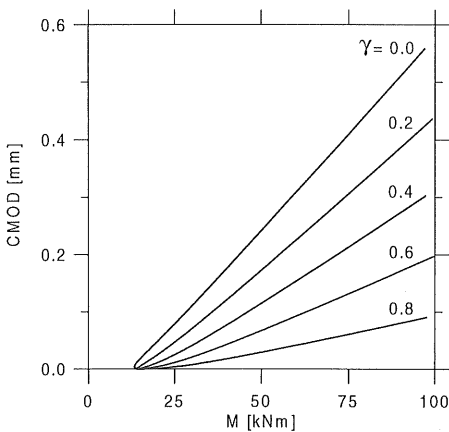
9 ACKNOWLEDGEMENT

Figure 7. Crack opening at the bottom face of the sample beam ($\rho = 0$). $CMOD$ plotted against the absolute moment, M, for different values of the toughness class, γ.

REFERENCES

Hillerborg, A., Modéer, M. & Petersson, P. 1976. Analysis of crack formation and crack growth in concrete by means of fracture mechanics and finite elements, *Cem. Concr. Res.* 6(6): 773-782.
Hillerborg, A. 1980. Analysis of fracture by means of the fictitious crack model, particularly for fibre reinforced concrete, *Int. J. Cem. Comp.* 2(4): 177-184.
Olesen, J.F. 2000. Cracks in reinforced FRC beams. In J.F. Olesen (ed.), *Papers in structural engineering and materials – a centenary celebration*, Department of Structural Engineering and Materials, Technical University of Denmark, pp. 211-220.
Rossi, P. 1995. Les betons de fibre metalliques. Final report on Beton de Fibres Metalliques, elements de structure functionnant comme de poutres by AFREM.

Stang, H. & Olesen, J.F. 1998. On the Interpretation of Bending Tests on FRC-Materials, *Fracture Mechanics of Concrete Structures, Proceedings FRAMCOS-3*, Aedificatio Publishers, D-79104, Freiburg, Germany, Vol. 1: 511-520

Stang, H. & Olesen, J.F. 2000. A Fracture Mechanics based Design Approach to FRC, *BEFIB 2000, Fifth RILEM Symposium on Fibre-Reinforced Concretes (FRC)*, RILEM Publications, France, PRO 15, pp. 315-324.

Vandewalle, L. 2000. Cracking behaviour of concrete beams reinforced with a combination of ordinary reinforcement and steel fibers, *RILEM Mat. and Struct.* Vol. 33, pp. 164-170.